CASL-U-2016-1069-000
ORNL/TM-2016/153

Subgroup Benchmark Calculations for the Intra-Pellet Nonuniform Temperature Cases

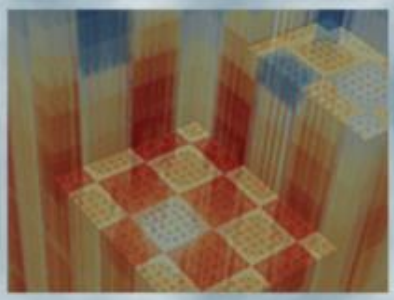
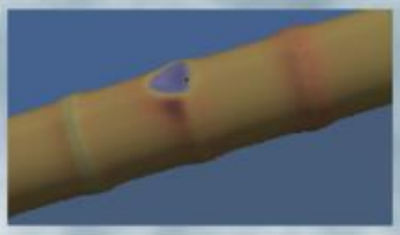
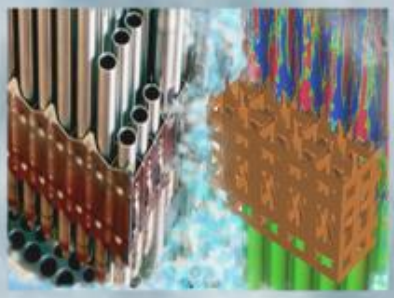

Revision 0
August 1, 2016

Kang Seog Kim
Yeon Sang Jung
Yuxuan Liu
Han Gyu Joo

U.S. DEPARTMENT OF ENERGY | Nuclear Energy

REVISION LOG

Revision	Date	Affected Pages	Revision Description
0	08/01/2016	All	Initial version

Document pages that are:

Export Controlled None

IP/Proprietary/NDA Controlled None

Sensitive Controlled None

Unlimited - All

Requested Distribution:

To: N/A

Copy: N/A

Reviewed by:

Date:

Reviewer: Kevin T. Clarno, Mark L. Williams

EXECUTIVE SUMMARY

A benchmark suite has been developed by Seoul National University (SNU) for intra-pellet nonuniform temperature distribution cases based on the practical temperature profiles according to the thermal power levels. Though a new subgroup capability for nonuniform temperature distribution was implemented in MPACT, no validation calculation has been performed for the new capability. This study focuses on benchmarking the new capability through a code-to-code comparison. Two continuous-energy Monte Carlo codes, McCARD and CE-KENO, are engaged in obtaining reference solutions, and the MPACT results are compared to the SNU nTRACER using a similar cross section library and subgroup method to obtain self-shielded cross sections.

CONTENTS

FIGURES

TABLES

ACRONYMS

CASL	Consortium for Advanced Simulation of Light Water Reactors
ORNL	Oak Ridge National Laboratory
SNU	Seoul National University
T/H	Thermal Hydraulic

1. INTRODUCTION

High-fidelity reactor simulations require a resonance self-shielding model to be able to resolve the spatial variation of the effective cross section within the fuel rod. If the thermal feedback is also considered, the resonance method should also be able to account for the nonuniform temperature distribution along the fuel radius. In the conventional lattice calculation, a so-called "effective temperature" is chosen to replace the realistic temperature distribution in the fuel rod so that the subgroup method can be performed without any extension for the nonuniform temperature case. Apparently, the effective temperature model cannot be used for the case of radially dependent temperature if one wants to obtain accurate self-shielded cross sections in every sub-region of the fuel for direct transport calculation.

However, the conventional subgroup methodology limits its application to the cases of uniform temperature distribution. The subgroup levels for different temperatures are identical, and the weights are generated to be different to account for the Doppler broadening of cross sections. When performing subgroup calculation for a nonuniform temperature case, for each subgroup, the subgroup levels for a resonance isotope in different fuel annuli are same, in spite of the different temperatures. This imposes an inconsistency with the real physics that the cross section should be Doppler broadened when temperature is increased. Therefore, the equivalence cross section calculated by the temperature-independent subgroup levels is biased. A solution to this deficiency is to adjust the cross section of each region with temperature dependence, so that the correct self-shielding effect can be retrieved.

A benchmark suite has been developed by Seoul National University (SNU) for the intra-pellet nonuniform temperature distribution cases based on the practical temperature profiles according to the thermal power levels. Though a new subgroup capability for nonuniform temperature distribution was implemented into MPACT [Joo04, Wem07, Liu04], no validation calculation has been performed for the new capability. This study focuses on benchmarking the new capability through a code-to-code comparison. Two continuous-energy Monte Carlo codes, McCARD and CE-KENO, are engaged in obtaining reference solutions with the ENDF/B-7.0 library, and the MPACT results are compared to the SNU nTRACER using a similar cross section library and subgroup method to obtain self-shielded cross sections.

2. METHODOLOGY

In a heterogeneous system, the self-shielded resonance cross sections are estimated from the self-shielded scalar fluxes obtained by the following fixed source transport equation.

$$\hat{\Omega}\cdot\nabla\psi_{g,m}+\sum_i(\Sigma_{i,a,g,m}+\lambda_{i,g}\Sigma_{i,p})\psi_{g,m}(\hat{\Omega})=\sum_i\lambda_{i,g}\Sigma_{i,p}\,, \tag{2.1}$$

where subscript *m* denotes a problem case with different absorption cross section levels at energy group *g*. In Eq. (2.1), $\Sigma_{i,a,g,m}$ and $\Sigma_{i,p}$ denote macroscopic absorption and potential cross sections of nuclide *i*, respectively, and $\lambda_{i,g}$ denotes the intermediate resonance parameter.

Eq. (2.1) should be modified for the resonance transport calculations involving nonuniform temperature distribution in which the macroscopic absorption cross sections should include the temperature distribution as follows:

$$\Sigma_{i,a,g,m}=N_i\sigma_{i,a,g,m}(T_{ave.})\frac{\sigma_{i,a,g,m}(T)}{\sigma_{i,a,g,m}(T_{ave.})}\approx N_i\sigma_{i,a,g,m}(T_{ave.})\,f_{i,a,g}(T)\,, \tag{2.2}$$

where *T* and $T_{ave.}$ are local and volume-averaged temperatures, respectively. The function *f(T)* was approximated by the following equation [Wem07].

$$f_{i,a,g}(T)=\frac{R_{i,a,g}(T,\sigma_p)}{R_{i,a,g}(T_{ave.},\sigma_p)}\cdot\frac{\sigma_p-R_{i,a,g}(T_{ave.},\sigma_p)}{\sigma_p-R_{i,a,g}(T,\sigma_p)}\,, \tag{2.3}$$

where

$$\sigma_p\approx\frac{\sum_{j=all}N_j\lambda_{j,g}\sigma_{j,p}}{N_i}\,. \tag{2.4}$$

Effective self-shielded absorption and ν*fission cross section can be obtained by the following equations.

$$\sigma_{i,a,g}=\frac{\sum_m w_{a,g,m}(T_j)\sigma_{i,a,g,m}\dfrac{\sigma_{b,g,m}}{\sigma_{i,a,g,m}f_{i,a,g}(T_j)+\sigma_{x,g}+\sigma_{b,g,m}}}{\sum_m w_{a,g,m}(T_j)\dfrac{\sigma_{b,g,m}}{\sigma_{i,a,g,m}f_{i,a,g}(T_j)+\sigma_{x,g}+\sigma_{b,g,m}}}\,, \tag{2.5}$$

$$\sigma_{i,vf,g}=\frac{\sum_m w_{vf,g,m}(T_j)\sigma_{i,vf,g,m}\dfrac{\sigma_{b,g,m}}{\sigma_{i,a,g,m}f_{i,a,g}(T_j)+\sigma_{x,g}+\sigma_{b,g,m}}}{1-\sum_m w_{a,g,m}(T_j)\dfrac{\sigma_{a,g,m}}{\sigma_{i,a,g,m}f_{i,a,g}(T_j)+\sigma_{x,g}+\sigma_{b,g,m}}}\,. \tag{2.6}$$

The SNU simulator nTRACER utilizes a different formula to obtain an effective self-shielded absorption cross section by using average temperature weights instead as follows:

$$\sigma_{i,a,g} = \frac{\sum_m w_{a,g,m}(T_{ave.}) f_{i,a,g}(T_j)\sigma_{i,a,g,m} \dfrac{\sigma_{b,g,m}}{\sigma_{i,a,g,m} f_{i,a,g}(T_j) + \sigma_{x,g} + \sigma_{b,g,m}}}{\sum_m w_{a,g,m}(T_{ave.}) \dfrac{\sigma_{b,g,m}}{\sigma_{i,a,g,m} f_{i,a,g}(T_j) + \sigma_{x,g} + \sigma_{b,g,m}}} . \quad (2.7)$$

3. SPECIFICATIONS

SNU has developed a benchmark suite for the intra-pellet nonuniform temperature distribution cases. Table 3.1 and Figure 3.1 provide the geometrical specifications, including five equi-volume subzones in the fuel pellet, gap, cladding, and moderator. Table 3.2 provides the compositional specification, including nuclides and atomic number densities.

Nonuniform temperature profiles as a function power and average fuel temperatures are shown in Table 3.3 and Figure 3.2. Benchmark calculations are performed by using both nonuniform and uniform temperature profiles.

Table 3.1. Geometrical data

Region	Dimensions		
Fuel	Outer Radius (cm)		0.4127
	Sub-pellet annular ring radius (cm)	1	0.1846
		2	0.2610
		3	0.3197
		4	0.3692
		5	0.4127
Gap			
Clad	Inner Radius (cm)		0.4203
	Outer Radius (cm)		0.4862
Coolant	Cell Pitch (cm)		1.2870

Table 3.2. Composition data

Composition	Nuclides		Atomic Number Density (atoms/barn-cm)
3.0 % UO_2	^{235}U	92235	7.13479E-04
	^{238}U	92238	2.27778E-02
	^{16}O	8016	4.69825E-02
Gap	^{16}O	8016	1.00000E-08
Clad	^{90}Zr	40090	2.22157E-02
	^{91}Zr	40091	4.79136E-03
	^{92}Zr	40092	7.24405E-03
	^{94}Zr	40094	7.18475E-03
	^{96}Zr	40096	1.13334E-03
Coolant	^{1}H	1001	4.65690E-02
	^{16}O	8016	2.32840E-02

Table 3.3. Nonuniform temperature profiles as a function power

Region		Temperature (K)						
		Power Level (%)						
		50	75	100	125	150	175	200
Pellet	1	787.4	897.7	1017.9	1148.2	1288.2	1437.7	1596.3
	2	754.7	843.7	939.3	1041.7	1150.6	1266.0	1387.5
	3	723.1	792.2	865.1	942.0	1022.7	1107.3	1195.6
	4	683.0	728.3	774.9	823.2	873.0	924.3	977.1
	5	669.2	708.3	748.4	789.4	831.4	874.3	918.2
	Avg.	723.5	794.0	869.1	948.9	1033.2	1121.9	1214.9
Gap		606.1	610.2	614.0	617.7	621.2	624.7	628.1
Clad		606.1	610.2	614.0	617.7	621.2	624.7	628.1
Coolant		586.7	586.7	586.7	586.7	586.7	586.7	586.7

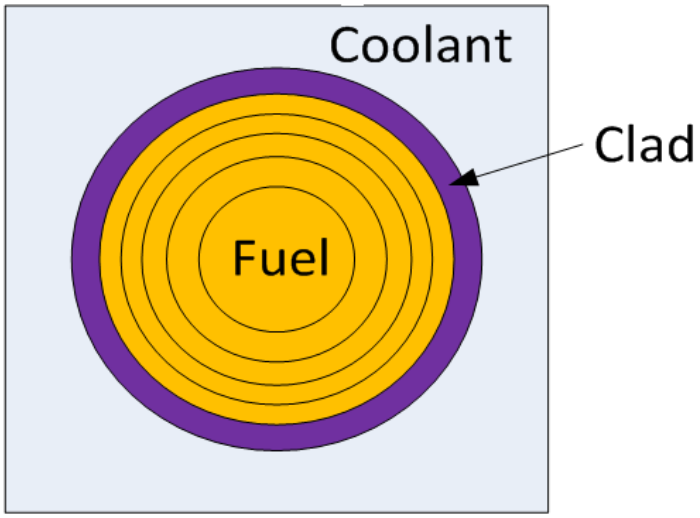

Figure 3.1. Geometrical configuration.

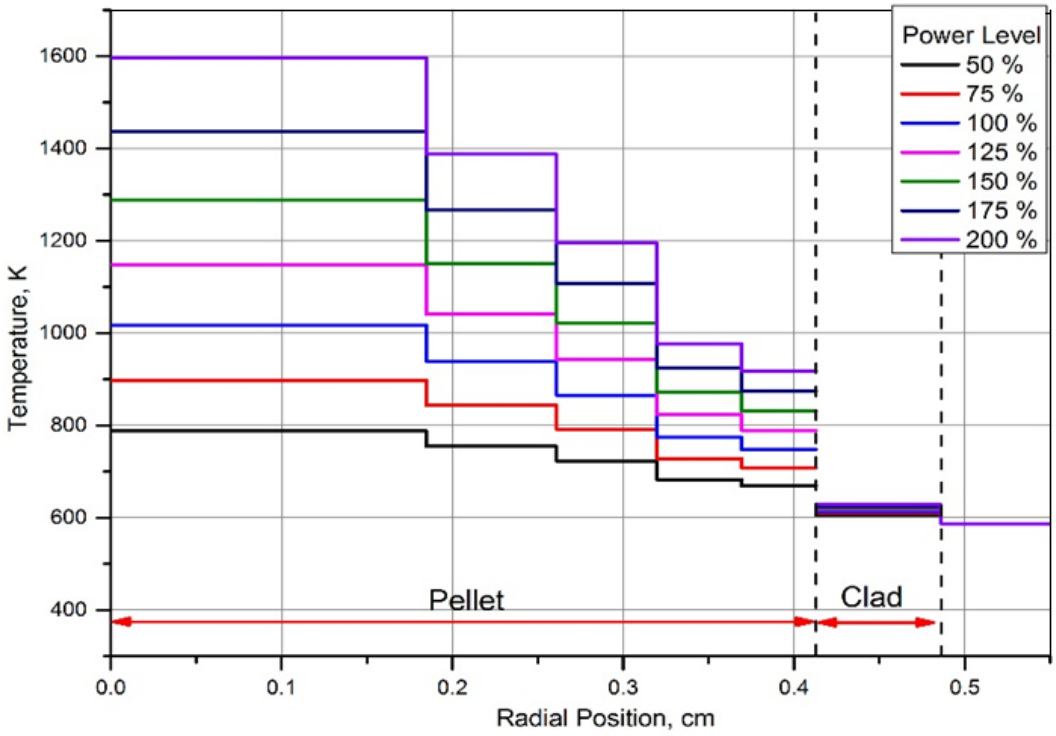

Figure 3.2. Nonuniform temperature profiles.

4. BENCHMARK RESULTS

Benchmark calculations were performed using the continuous-energy Monte Carlo codes McCARD and CE-KENO and the deterministic neutronic simulators nTRACER and MPACT with its own ENDF/B-7.0 continuous-energy and 47-group cross section libraries. The ACE format continuous-energy cross sections for McCARD were processed for all temperatures by NJOY. The SCALE-6.2 with CE-KENO includes a new capability to interpolate continuous-energy cross sections for any specified temperature based on the reference temperatures for base cross sections. However, if the specified temperature differs from the reference temperature within 4 K, no interpolation will be made.

Figure 4.1 provides a comparison of reactivities between nonuniform and uniform temperature results obtained by McCARD for which the ACE format continuous-energy cross sections were processed for all temperatures by using NJOY. This comparison indicates that the slopes of nonuniform and uniform temperatures, which indicate the fuel temperature coefficients, are different. In other words, the fuel temperature coefficient of the nonuniform temperature is less negative than that of the uniform temperature. Therefore, when performing whole core calculations with thermal/hydraulic (T/H) feedback, nonuniform temperature profiles need to be considered properly in estimating resonance self-shielded cross sections by performing subgroup calculations.

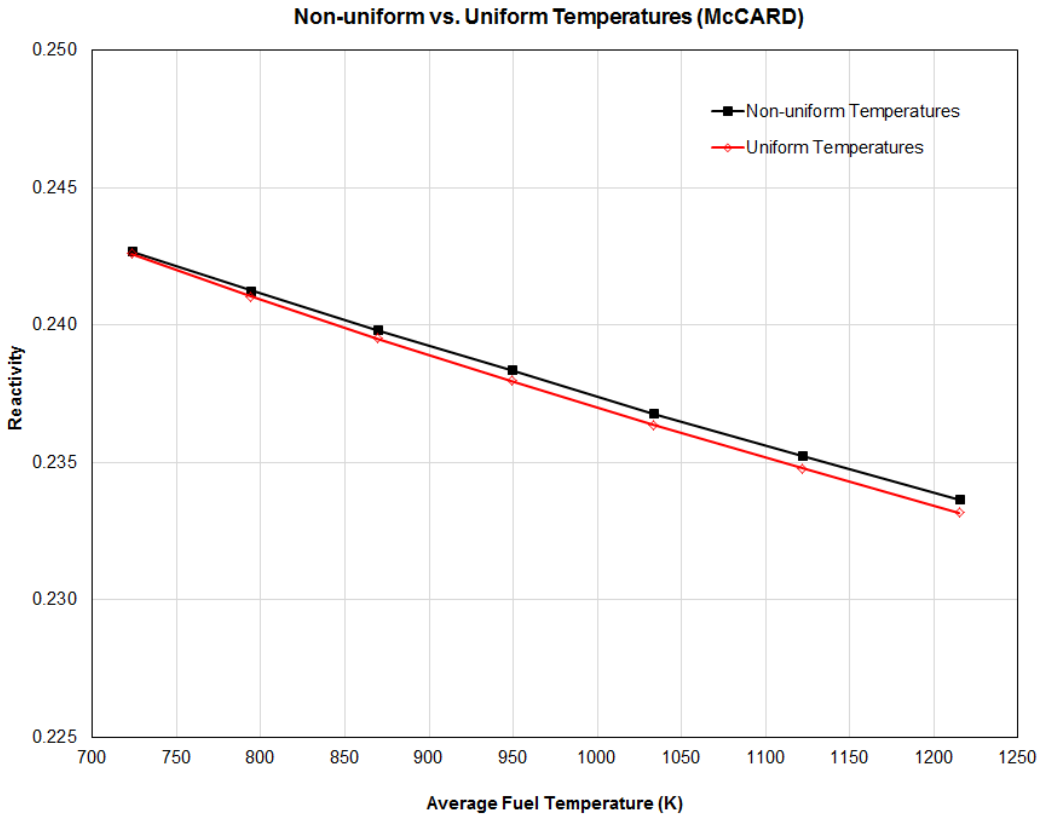

Figure 4.1. Comparison of reactivities between nonuniform and uniform temperature distributions.

Table 4.1 and Figure 4.2 provide the benchmark results for the uniform temperature cases. There is very good agreement among all codes in the reactivities for all temperatures. However, the slopes (fuel temperature coefficients) are somewhat different. The difference between the two Monte Carlo codes needs to be determined.

Table 4.1. Benchmark results for the uniform temperature distributions

Code	Power (%)	Fuel Temp. (K)	k-inf	STD (pcm)	Reactivity	Δρ (pcm)
McCARD	50	723.5	1.32032	3	0.24261	-
	75	794.0	1.31759	3	0.24104	-
	100	869.1	1.31494	3	0.23951	-
	125	948.9	1.31230	3	0.23798	-
	150	1033.2	1.30955	3	0.23638	-
	175	1121.9	1.30682	3	0.23478	-
	200	1214.9	1.30408	3	0.23318	-
nTRACER	50	723.5	1.32006	-	0.24246	-14.9
	75	794.0	1.31732	-	0.24088	-15.6
	100	869.1	1.31453	-	0.23927	-23.7
	125	948.9	1.31171	-	0.23764	-34.3
	150	1033.2	1.30886	-	0.23598	-40.3
	175	1121.9	1.30596	-	0.23428	-50.4
	200	1214.9	1.30298	-	0.23253	-64.7
MPACT	50	723.5	1.31925	-	0.24200	-61.3
	75	794.0	1.31659	-	0.24046	-57.7
	100	869.1	1.31389	-	0.23890	-61.0
	125	948.9	1.31105	-	0.23725	-72.8
	150	1033.2	1.30812	-	0.23555	-83.4
	175	1121.9	1.30518	-	0.23382	-96.4
	200	1214.9	1.30220	-	0.23207	-110.8
CE-KENO	50	723.5	1.31939	20	0.24207	-53.4
	75	794.0	1.31651	13	0.24042	-62.3
	100	869.1	1.31380	13	0.23885	-66.0
	125	948.9	1.31111	13	0.23729	-69.2
	150	1033.2	1.30827	13	0.23563	-74.7
	175	1121.9	1.30536	16	0.23393	-85.6
	200	1214.9	1.30263	11	0.23232	-85.4

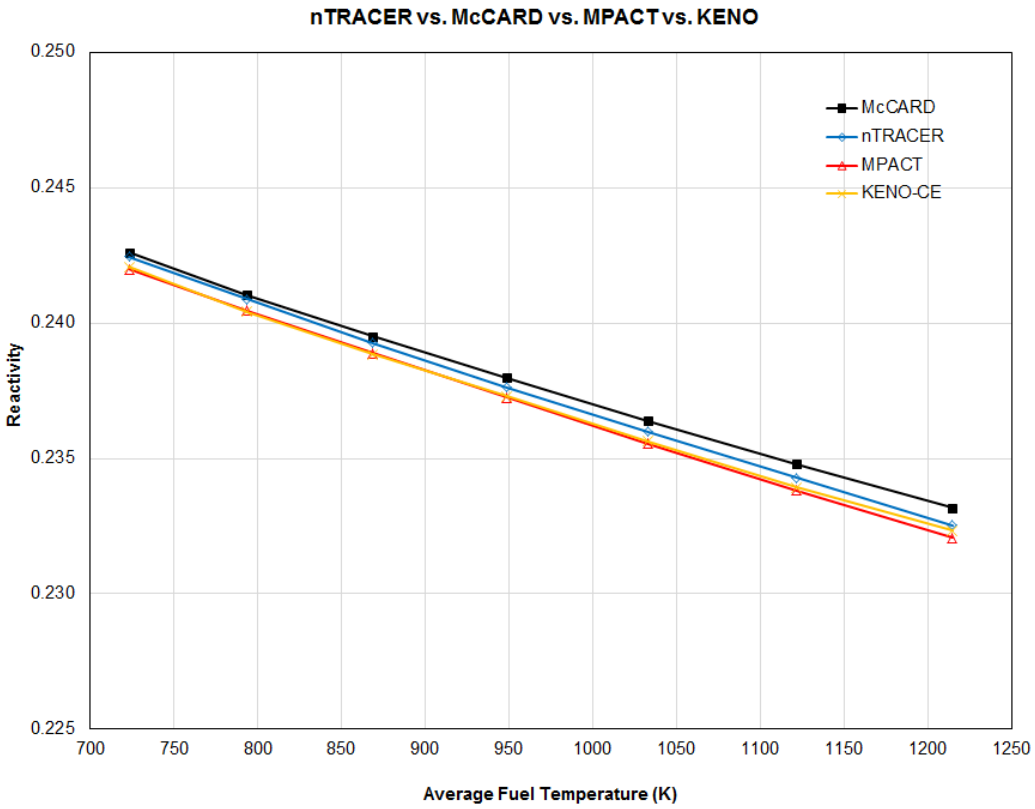

Code	Fuel Temp. Coeff. (pcm/K)	[a]-[b] or [a]-[c] (%)	[b]-[a] or [b]-[c] (%)
McCARD[a]	-1.934	-	-3.6
CE-KENO[b]	-2.004	3.5	-
nTRACER[c]	-2.033	4.8	1.4
MPACT[c]	-2.030	4.7	1.2

Figure 4.2. Comparison of reactivities for the uniform temperature distributions.

Table 4.2 and Figure 4.3 provide the benchmark results for the nonuniform temperature cases. There is very good agreement among all codes in the reactivities for all temperatures. This difference may be the result of cross section interpolation, the error source of which needs to be determined. The difference between MPACT and nTRACER may the result of differences in subgroup data and other cross sections and the nonuniform temperature subgroup equation.

Table 4.2. Benchmark results for the nonuniform temperature distributions

Code	Power (%)	Fuel Temp. (K)	k-inf	STD (pcm)	Reactivity	Δρ (pcm)
McCARD	50	723.5	1.32046	3	0.24269	-
	75	794.0	1.31798	3	0.24126	-
	100	869.1	1.31551	3	0.23984	-
	125	948.9	1.31298	3	0.23837	-
	150	1033.2	1.31027	3	0.23680	-
	175	1121.9	1.30760	3	0.23524	-
	200	1214.9	1.30491	3	0.23366	-
nTRACER	50	723.5	1.32026	-	0.24257	-11.5
	75	794.0	1.31763	-	0.24106	-20.2
	100	869.1	1.31497	-	0.23953	-31.2
	125	948.9	1.31228	-	0.23797	-40.6
	150	1033.2	1.30956	-	0.23638	-41.4
	175	1121.9	1.30681	-	0.23478	-46.2
	200	1214.9	1.30400	-	0.23313	-53.5
MPACT	50	723.5	1.31993	-	0.24239	-30.2
	75	794.0	1.31763	-	0.24106	-20.3
	100	869.1	1.31521	-	0.23966	-17.4
	125	948.9	1.31268	-	0.23820	-17.1
	150	1033.2	1.31011	-	0.23670	-9.6
	175	1121.9	1.30750	-	0.23518	-6.0
	200	1214.9	1.30487	-	0.23364	-2.2
CE-KENO	50	723.5	1.31932	7	0.24203	-65.6
	75	794.0	1.31679	6	0.24058	-68.3
	100	869.1	1.31420	7	0.23908	-75.9
	125	948.9	1.31147	8	0.23749	-87.5
	150	1033.2	1.30878	8	0.23593	-86.8
	175	1121.9	1.30609	7	0.23435	-88.7
	200	1214.9	1.30337	7	0.23276	-90.0

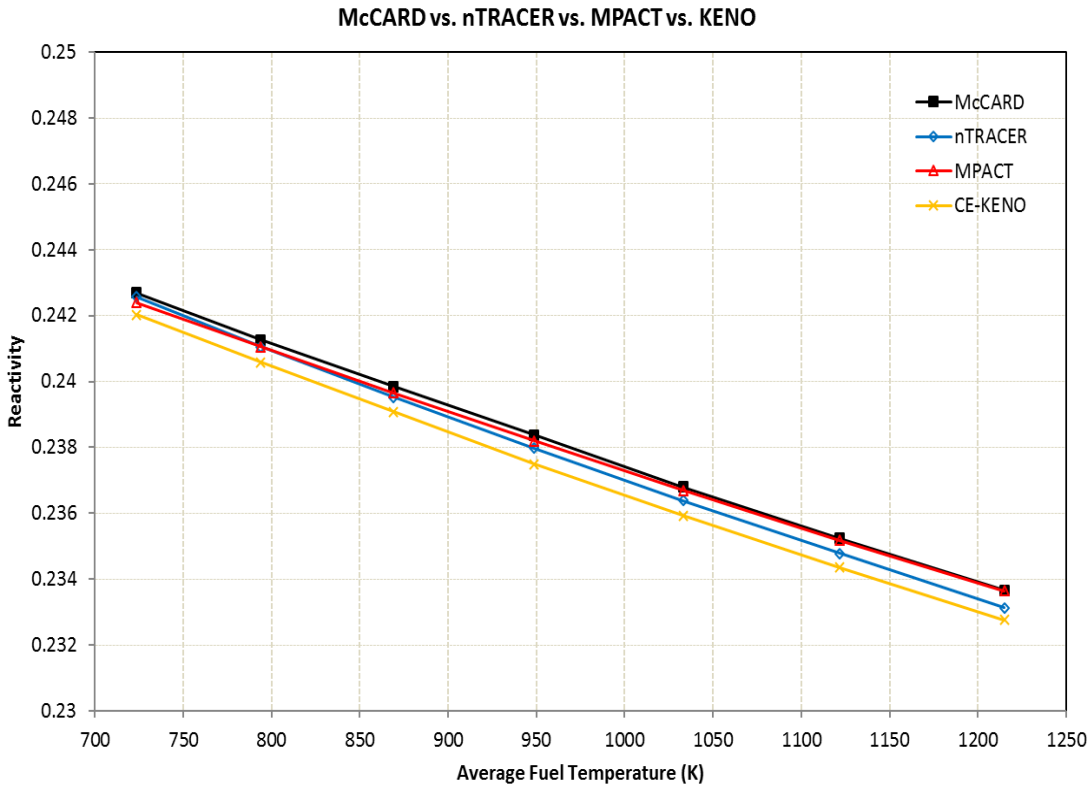

Code	Fuel Temp. Coeff. (pcm/K)	[a]-[b] or [a]-[c] (%)	[b]-[a] or [b]-[c] (%)
McCARD[a]	-1.847	-	-2.8
CE-KENO[b]	-1.899	2.7	-
nTRACER[c]	-1.933	4.5	-1.8
MPACT[c]	-1.788	-3.3	-6.2

Figure 4.3. Comparison of reactivities for the nonuniform temperature distributions.

5. DISCUSSION AND CONCLUSION

Benchmark calculations were performed for the intra-pellet uniform and nonuniform temperature distribution cases using the two-continuous energy Monte Carlo codes McCARD and CE-KENO and the deterministic transport codes MPACT and nTRACER with their own 47-group cross section libraries including subgroup data. Subgroup formulas used in MPACT and nTRACER are working reasonably. However, several pending technical issues require further investigation in this benchmark calculations including the following:

a. reactivity differences between McCARD and CE-KENO,
b. the non-physical reactivity shapes of CE-KENO for the nonuniform temperature cases,
c. the difference between MPACT and nTRACER when using same cross section library and same equation in MPACT and nTRACER, and
d. comparison of 1-group total and nuclide-wise reaction rates at each pellet sub-zone.

ACKNOWLEDGMENT

The authors greatly appreciate the valuable comments provided by the technical reviewers of this documents.

REFERENCES

[Joo05] H. G. Joo, B. S. Han, C. H. Kim, Kang Seog Kim, "Implementation of Subgroup Method in Direct Whole Core Transport Calculation Involving Nonuniform Temperature Distribution," M&C 2005, Avignon, France, Sept. 12–15, 2005 (2005)

[Wem07] C. A. Wemple, R. J. J. Stamm'ler, and A. A. Ferri, "Improved Temperature-Dependent Resonance Treatment in HELIOS-1.9," *Trans. Am. Nucl. Soc.*, **96**, 657 (2007)

[Liu04] Yuxuan Liu, Kang Seog Kim, "Implementation of Non-Uniform Temperature Treatment Capability for Subgroup Method," CASL-X-2014-PHI.VCS.P9.03-006 Rev.0 (2014)

APPENDIX A. THE MPACT INPUT FILE

[Geometry input file]

```
!Ray tracing module dimensions
 mod_dim 1.2870 1.2870 1.0

 !Pin mesh
  pinmesh 1 cyl  0.1846 0.2610 0.3197 0.3692 0.4127 0.4203 0.4862 0.575 / 1.2870 / 1.0 / 8*1 /
9*8 /  1  !Pin mesh

!  Material 1:  Fuel
!  Material 2:  Fuel
!  Material 3:  Fuel
!  Material 4:  Fuel
!  Material 5:  Fuel
!  Material 6:  Gap
!  Material 7:  Clad
!  Material 8:  Water

 pin 1 1 / 1 2 3 4 5 6 7 8 8

!Pin modular ray tracing
 module 1 3*1
1
```

[Main input file]

```
CASEID Case_01

MATERIAL
  mat  1 2 10.36 g/cc 787.4 K  \ 92235 7.13479E-04
                               92238 2.27778E-02
                                8001 4.69825E-02
  mat  2 2 10.36 g/cc 754.7 K  \ 92235 7.13479E-04
                               92238 2.27778E-02
                                8001 4.69825E-02
  mat  3 2 10.36 g/cc 723.1 K  \ 92235 7.13479E-04
                               92238 2.27778E-02
                                8001 4.69825E-02
  mat  4 2 10.36 g/cc 683.0 K  \ 92235 7.13479E-04
                               92238 2.27778E-02
                                8001 4.69825E-02
  mat  5 2 10.36 g/cc 669.2 K  \ 92235 7.13479E-04
                               92238 2.27778E-02
                                8001 4.69825E-02
  mat  6 0 0.001 g/cc 600 K    \  8001 1.00000E-06
  mat  7 4 6.56  g/cc 606.1 K  \ 40090 2.22157E-02
                               40091 4.79136E-03
                               40092 7.24405E-03
                               40094 7.18475E-03
                               40096 1.13334E-03
  mat  8 0 0.661 g/cc 586.7 K  \  1001 4.65690E-02
                                8016 2.32840E-02

GEOM

 !Loads pin modular ray tracing and all pin types
 !Module 1 - common pin geometry

 file base_bench1_geom.inp

 !Define lattices, assemblies and core
 lattice 1 2*1
  1

 assembly 1
  1
```

```
 core 360
  1

XSEC
  addpath .
  xslib ORNL mpact47g_70s_v4.1m3_03192015.fmt

OPTION
  bound_cond 1 1 1 1 1 1
  solver 1 2
  ray 0.02 CHEBYSHEV-YAMAMOTO 16 3
  !parallel 1 1 1 16
  conv_crit 2*1.e-6
  iter_lim 2000 2 3
  scatt_meth  P2
  vis_edits F
  validation T C
```

APPENDIX B. THE CE-KENO INPUT FILE

```
=csas6
centrm verification pincell c01
ce_v7.0_endf
read comp
' Fuel-1
u-235 1 0  7.13479E-04   787.4  end
u-238 1 0  2.27778E-02   787.4  end
o-16  1 0  4.69825E-02   787.4  end
' Fuel-2
u-235 2 0  7.13479E-04   754.7  end
u-238 2 0  2.27778E-02   754.7  end
o-16  2 0  4.69825E-02   754.7  end
' Fuel-3
u-235 3 0  7.13479E-04   723.1  end
u-238 3 0  2.27778E-02   723.1  end
o-16  3 0  4.69825E-02   723.1  end
' Fuel-4
u-235 4 0  7.13479E-04   683.0  end
u-238 4 0  2.27778E-02   683.0  end
o-16  4 0  4.69825E-02   683.0  end
' Fuel-5
u-235 5 0  7.13479E-04   669.2  end
u-238 5 0  2.27778E-02   669.2  end
o-16  5 0  4.69825E-02   669.2  end
' Gab
o-16  6 0  1.00000E-06   600.0  end
' Clad
zr-90 7 0  2.22157E-02   606.1  end
zr-91 7 0  4.79136E-03   606.1  end
zr-92 7 0  7.24405E-03   606.1  end
zr-94 7 0  7.18475E-03   606.1  end
zr-96 7 0  1.13334E-03   606.1  end
' h2o
h-1   8 0  4.65690E-02   586.7  end
o-16  8 0  2.32840E-02   586.7  end
end comp

read parm
  gen=200 npg=200000 nsk=100  scx=no
end parm

read geom
global unit 10
cylinder 11 0.18460 chord +x=0.0 chord +y=0.0
cylinder 12 0.26100 chord +x=0.0 chord +y=0.0
cylinder 13 0.31970 chord +x=0.0 chord +y=0.0
cylinder 14 0.36920 chord +x=0.0 chord +y=0.0
cylinder 15 0.41270 chord +x=0.0 chord +y=0.0
cylinder 16 0.42030 chord +x=0.0 chord +y=0.0
cylinder 17 0.48620 chord +x=0.0 chord +y=0.0
cuboid 18 0.64350 0.0 0.64350 0.0 5.0 -5.0
media 1 1 11
media 2 1 12 -11
media 3 1 13 -12
media 4 1 14 -13
media 5 1 15 -14
media 6 1 16 -15
media 7 1 17 -16
media 8 1 18 -17
boundary 18
end geom

read bounds
all=refl
end bounds

end data
end
```